Supplementary Information for:

Exploring Electrochemical Performance of Layered Bi_2Se_3 Hexagonal Platelets as Anode Material for Lithium-Ion Batteries

Shaik M. Abzal [a ‡], Sumit Khatua [a‡], Kurapati Kalyan [a], Sai Lakshmi Janga [a], Rajkumar Patel [b,*], L.N. Patro [a,*], Jatis Kumar Dash [a,*]

[a] *Department of Physics, SRM University-AP, Amaravati 522240, India.*

[b] *Energy and Environmental Science and Engineering (EESE), Integrated Science and Engineering Division (ISED), Underwood International College, Yonsei University, Yeonsu-gu, Incheon 21983, South Korea.*

‡ These authors have equally contributed to this work.

*Corresponding Authors

E-mail: [JKD: jatis.d@srmap.edu.in, jatiskumar@gmail.com],

[LNP: laxminarayana.p@srmap.edu.in], [RP: rajkumar@yonsei.ac.kr]

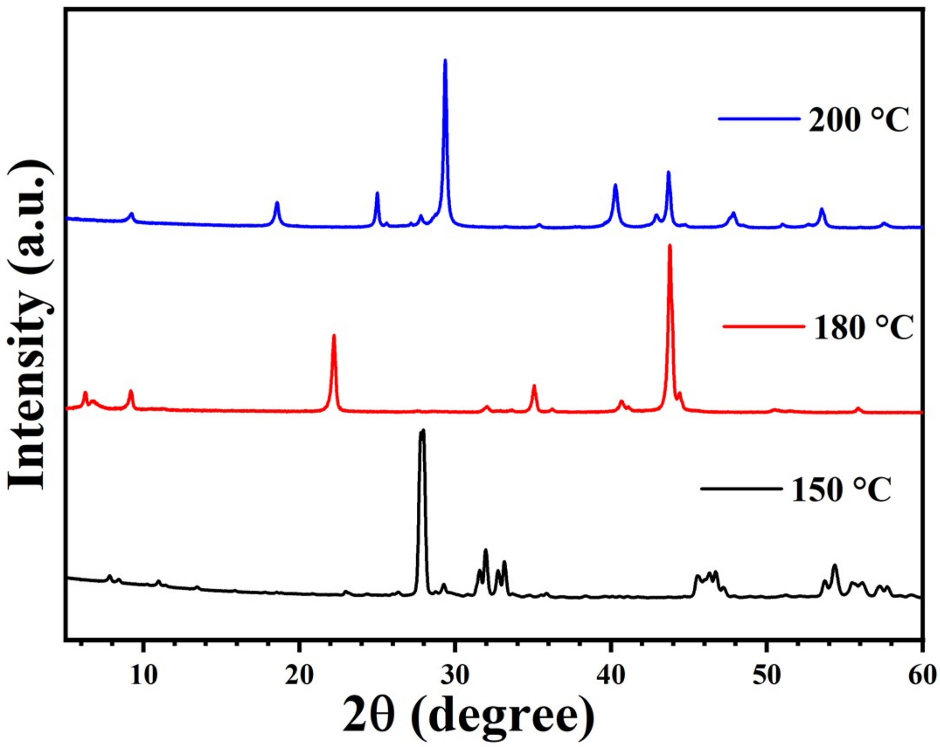

Fig S1. XRD patterns of Bi_2Se_3 at various synthesis temperatures.

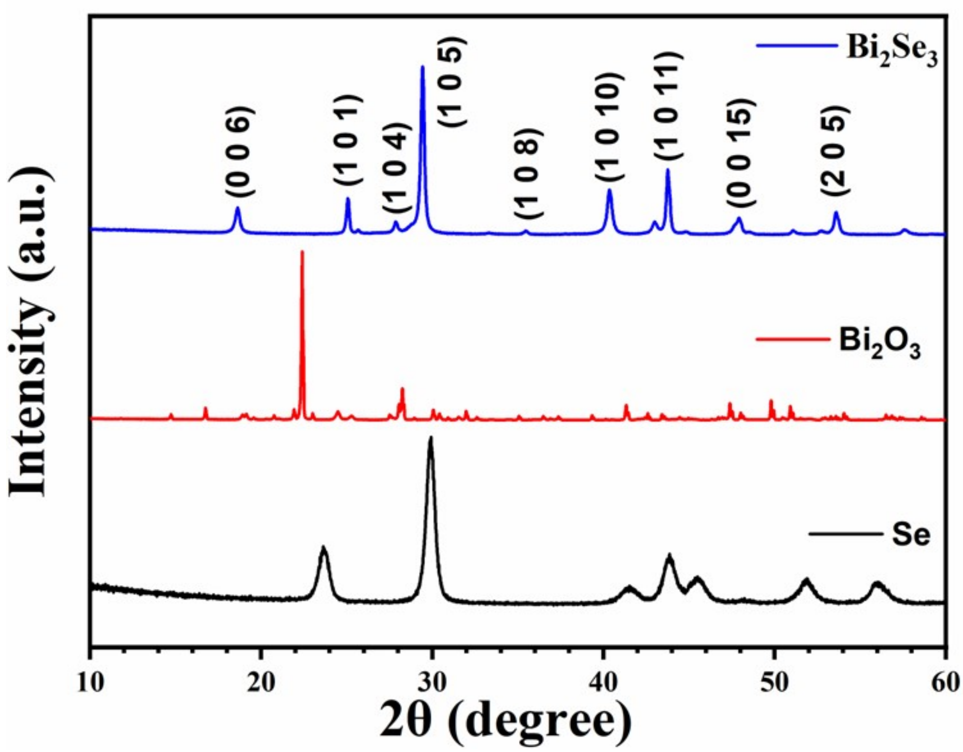

Fig S2. XRD pattern of Bi_2Se_3 with precursor material, Bi_2O_3 and Se.

S.no	Peak position (2θ °)	FWHM (rad)	Crystallite Size (nm)
1.	9.26	0.0052	26.3
2.	18.62	0.0055	25.2
3.	25.06	0.0032	43.5
4.	29.4	0.0044	32.1
5.	43.7	0.0041	35.6
Average crystallite size			32.5

Table S1. The Average crystallite size of the Bi_2Se_3.

The average crystallite size of the hexagonal Bi_2Se_3 is calculated by using the Debye-Scherrer equation, $D = \frac{k\lambda}{\beta \cos\theta}$, where k represents the Scherrer constant (k = 0.9), λ denotes the wavelength of X-rays used (1.54 Å), β refers to the full width at half maximum (FWHM) of the diffraction peak, and θ is the Bragg's angle.

Table S2. The morphology of Bi_2Se_3 reported by different synthesis methods.

Synthesis methods	Morphology	Reference
Template synthesis	Micropillars	1

Chemical vapor deposition	Triangular or hexagonal shape	2
Chemical vapor deposition	Nano wire &Nano ribbons	3
Microwave assisted	Nano Sheets	4
One-pot reaction	Nano dots	5

TEM EDX:

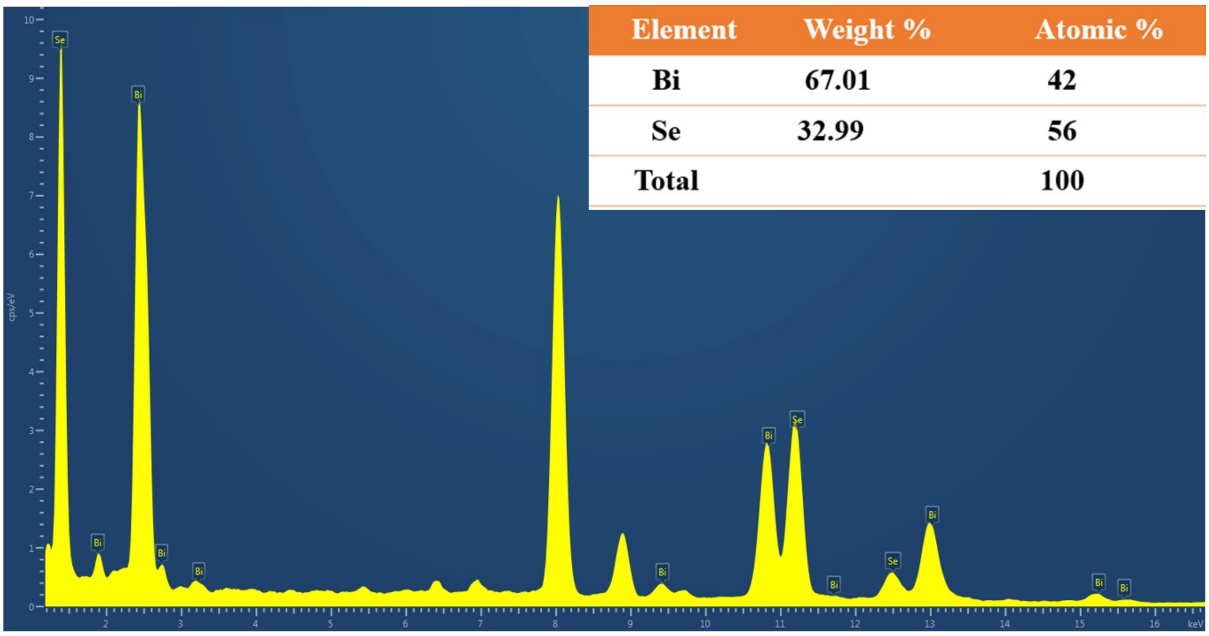

Fig S3. TEM (EDAX) *Energy-dispersive X-ray analysis* of Bi_2Se_3.

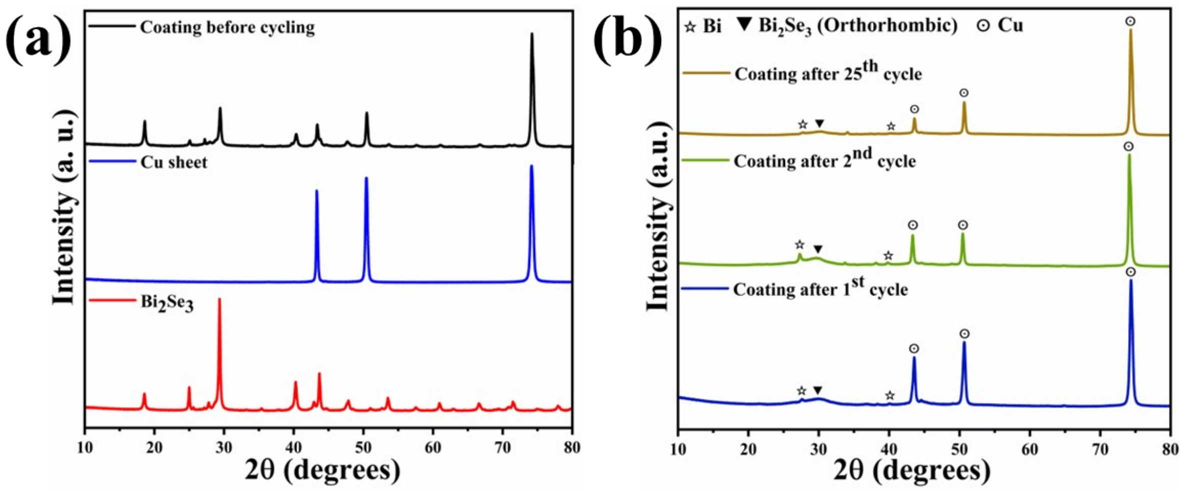

Fig S4. XRD pattern of (a) pure Bi_2Se_3, Cu sheet, Bi_2Se_3 coated on Cu sheet. (b) Bi_2Se_3 anode materials after 1st, 2nd, and 25th cycle (3V charging) coated on copper sheet.

Figure S4 (b) shows the XRD pattern of Bi_2Se_3 anode materials after 1st, 2nd, and 25th cycle (3V charging) coated on copper sheet. As shown in figure, the sharp peak at 43.5, 50.7, and 74.2° correspond to the peak due to copper sheet.

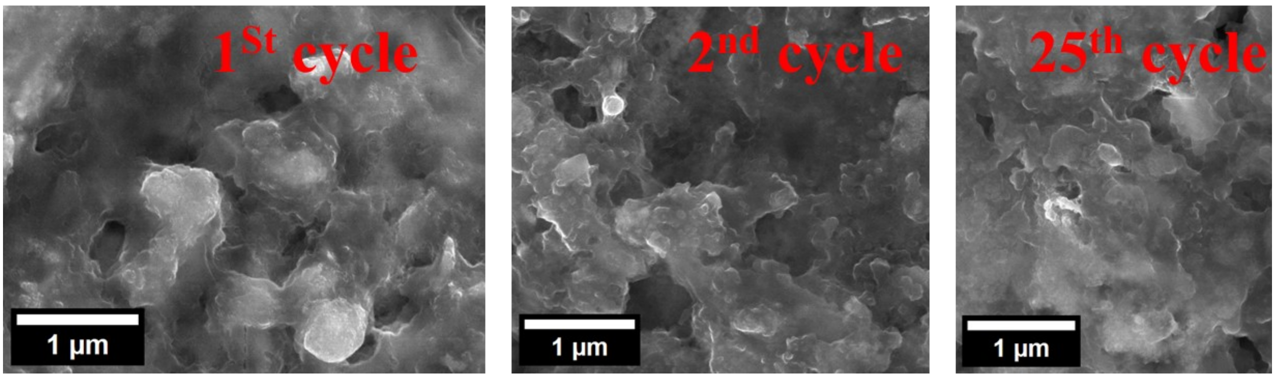

Fig S5. Surface morphology of Bi_2Se_3 after (a) 1st cycle Cu sheet, Bi_2Se_3 coated on Cu sheet. (b), 2nd cycle, (c) 25th cycle.

Reference:

(1) Klösel, K.; Pané, S.; Mihailovic, I. A.; Hierold, C. Template-assisted electrosynthesis of thick stoichiometric thermoelectric Bi 2 Se 3 micropillars. *Electrochimica Acta* **2022**, *403*.

(2) Jiang, Y.; Zhang, X.; Wang, Y.; Wang, N.; West, D.; Zhang, S.; Zhang, Z. Vertical/planar growth and surface orientation of Bi2Te3 and Bi2Se3 topological insulator nanoplates. *Nano Lett.* **2015**, *15* (5), 3147–3152.

(3) Zou, Y.; Chen, Z. G.; Huang, Y.; Yang, L.; Drennan, J.; Zou, J. Anisotropic electrical properties from vapor-solid-solid grown Bi2Se3 nanoribbons and nanowires. *J. Phys. Chem. C* **2014**, *118* (35), 20620–20626.

(4) Xu, H.; Chen, G.; Jin, R.; Chen, D.; Wang, Y.; Pei, J.; Zhang, Y.; Yan, C.; Qiu, Z. Microwave-assisted synthesis of Bi2Se3 ultrathin nanosheets and its electrical conductivities. *CrystEngComm* **2014**, *16* (19), 3965–3970.

(5) Mao, F.; Wen, L.; Sun, C.; Zhang, S.; Wang, G.; Zeng, J.; Wang, Y.; Ma, J.; Gao, M.; Li, Z. Ultrasmall Biocompatible Bi2Se3 Nanodots for Multimodal Imaging-Guided Synergistic Radiophotothermal Therapy against Cancer. *ACS Nano* **2016**, *10* (12), 11145–11155.